



**ARTICLE**

## Desorption Behavior and Thermogravimetric Analysis of Bio-Hardeners

Benoit Ndiwe<sup>1,2,3</sup>, Antonio Pizzi<sup>4,\*</sup>, Hubert Chapuis<sup>5</sup>, Noel Konai<sup>6</sup>, Lionel Karga<sup>7</sup>, Pierre Girods<sup>4</sup> and Raidandi Danwe<sup>6,8</sup>

<sup>1</sup>Department of Mechanical Engineering, Higher Technical Teacher Training College Douala (ENSET), University of Douala, Douala, Cameroon

<sup>2</sup>Laboratory of Forest Resources and Wood Valorization (Larefob), ENSET of Douala, Douala, Cameroon

<sup>3</sup>Department of Engineering Science, West University, Trollhättan, Sweden

<sup>4</sup>LERMAB-ENSTIB, University of Lorraine, Epinal, 88051, France

<sup>5</sup>Laboratoire D'Etudes et de Recherche sur le Matériau Bois LERMAB, Faculté des Sciences et Technologies, Université de Lorraine, Nancy, France

<sup>6</sup>Laboratory of Materials Mechanics, Structures and Integrated Manufacturing, National Advanced School of Engineering, Yaoundé 1 University, Yaoundé, Cameroon

<sup>7</sup>Department of Mechanical Petroleum and Gas Engineering, Faculty of Mines and Petroleum Industries, University of Maroua, Kaélé, Cameroon

<sup>8</sup>Laboratory of Mechanic, Materials and Building, Sahel Institute of Maroua University, Maroua, Cameroon

\*Corresponding Author: Antonio Pizzi. Email: antonio.pizzi@univ-lorraine.fr

Received: 22 October 2021 Accepted: 27 December 2021

### ABSTRACT

In this work, the thermal degradation and drying of bio-hardeners are investigated. Four bio-hardeners based on exudates of *Senegalia senegal*, *Vachellia nilotica*, *Vachellia seyal*, and *Acacia siebteriana* were analyzed by FTIR and thermogravimetric analysis, and a desorption study was also conducted. The analysis by infrared spectroscopy indicates the existence of oligomers of different types all giving 5-hydroxy-2-hydroxymethylfuran and 2,5-dihydroxymethylfuran which are then the real hardening molecules. The pyrolysis of these extracts reveals three main regions of mass loss, a first region is located between 25°C and 110°C reflecting the loss of water from the adhesive and the formation of some traces of volatile organic compounds such as CO<sub>2</sub> and CO, a second zone characterized by the release of CO, CO<sub>2</sub> and CH<sub>4</sub> gases with peaks between 110° and 798.8°C. At the end of the analysis, about 22% of the initial mass remains undecomposed, this mass corresponds to the rigid segments of the bio-hardener which are not completely decomposed.

### KEYWORDS

Exudates; pyrolysis; FTIR; bio-hardener; desorption

### Nomenclature

CO	Carbon monoxide
CO <sub>2</sub>	Carbon dioxide
CH <sub>4</sub>	Methane
DTG	Derivative Thermogravimetry



FTIR	Fourier-transform infrared spectroscopy
MR	desorption ratio
R	correlation coefficient
T°	temperature
TG	Thermogravimetry

## 1 Introduction

Today, the demand for particleboard and plywood has grown exponentially. The cohesion of these materials has long been ensured by synthetic resins that are used as a matrix in the wood industry. However, there are many limitations: panels based on these adhesives are not water-resistant and emit formaldehyde which is dangerous for humans and their environment [1]. Indeed, formaldehyde is now classified as a carcinogen by the International Agency for Research on Cancer (CIRC 1995). As regards phenol-formaldehyde resins, these have a high cost, they discharge toxic phenols into the environment [2]. For this reason, even their use is starting to be questioned today. Isocyanate adhesives are also expensive, and the presence of unreacted, free isocyanate group is also unacceptable for public health reasons [3].

The fight against pollution caused using synthetic resins, as well as using those based on formaldehyde (a substance classified as carcinogenic), has led several researchers to develop environment-friendly bio-adhesives to bond wood [4]. Pichelin et al. [5]; were able to glue structural beams with formaldehyde combined with free tannin adhesives. In 2007, Liu et al. [6]; developed and characterized soy protein-based adhesives for wood bonding Konai et al. [7] developed bioadhesives based on *Aningre superba* tannin with 5.5% paraformaldehyde. Only from 2013 occurred successful preparation of a 100% bioadhesive from tannins using furfuryl alcohol [8] and from 2018 with hydroxymethylfurfural as a hardener [9]; lastly, Ndiwe et al. [10–12] produced for the first-time bio-adhesives using tannins and bio-hardeners from natural plants.

Compared to the new bio-based materials, wood-based materials bonded with traditional adhesives are still very extensively used by companies around the world. Most of these materials such as particleboard [13], plywood [14], medium density fiberboard [15], and oriented strand board [16] are prepared by gluing wood components with petroleum-derived adhesives. Urea-formaldehyde, melamine-formaldehyde, and phenol-formaldehyde resins are examples of such adhesives [17–20]. However, with the use of these resins comes the concern regarding volatile organic compound (VOC) emissions, potential health risks, and non-biodegradability [21–23]. Although isocyanate-based resins are used in the wood industry to avoid using formaldehyde, a great part of the raw materials for these adhesives are derived from non-renewable fossil resources, which continue to decline. These concerns have driven manufacturers of wood-based materials to focus research to establish product portfolios that contain more sustainable and environment-friendly products. Specifically, formaldehyde-free and renewable energy-based wood adhesives have become major topics of ongoing investigations [10,11,24–26].

To contribute to this objective, bio-adhesives using bio-hardeners from African plants have been shown today to be suitable for the preparation of particleboard [10–12].

It is, therefore, necessary to answer the question of the choice of hardeners for tannin resins without emission of formaldehyde while preparing panels of good mechanical resistance, which do not attack the environment, and which resist the attacks of insects and microbiological agents.

In this article, exudates used as bio-hardeners were extracted from tropical plants in Cameroon, Central Africa. Exudates are substances that ooze from the pores of diseased or damaged plant tissue, they are complex mixtures of organic compounds that are secreted into the extracellular matrix and normally appear on the plant surface [27], These substances have been harvested and used throughout history for

example as adhesives and coatings, thickeners, cosmetic ingredients, The Mayans were already harvesting latex from trees 1600 BC to make large rubber balls which they used to secure the connection between the head and handle of axes [28]. In addition, Egyptian hieroglyphs attest to the ancient use of exudates including gum arabic which has been traded for at least 4000 years [29]. Some exudates, however, have been valued for their medicinal uses, in particular for their antiseptic and anti-inflammatory properties [30].

They are characterized for their potential use as bio-hardeners in the wood industry. It is therefore of primary interest to determine the upper-temperature limits to which the bio-hardeners can be safely subjected, to determine their decomposition points and stiffnesses, and to study their drying kinetics. This operation allows: to use bio-hardeners whose moisture content is in hygroscopic balance with their environment of use, to obtain relatively stable works, deactivation of enzymes responsible for the degradation of natural products, inhibition of the growth of microorganisms through the reduction of water activity, and to reduce the risks of deterioration and disorders caused by the attack of fungi and other parasites. This paper presents the results of thermal and drying experiments of bio-hardeners exudates of *Vachellia nilotica*, *Vachelia seyal*, *Senegalia senegal*, and *Acacia siebteriana*.

## 2 Experimental

### 2.1 Extraction

Exudates of *Vachellia nilotica*, *Senegalia senegal*, *Vachelia seyal*, and *Acacia siebteriana* from the Dacheka forest in the far northern region of Cameroon were extracted. The *Vachellia nilotica* tree was wounded by incisions and from the wound emerged a complex organic solution of high viscosity called an exudate.

The locality of Dacheka is in the Far-North Cameroon region, a semi-arid Sahelian tropical region with an aridity index between 0.20 and 0.50 [31] his geographical coordinates are latitude: 10.1333, longitude: 14.9 10° 7' 60" North, 14° 54' 0" East. where it is extremely hot, with ambient temperatures reaching more than 40°C in March. This type of ecosystem is characterized by the non-availability of soil water with low rainfall, the annual rainfall being 811 mm. The harmattan wind blows from October to March. The heart of the dry season is in January. Southwest winds appear timidly in June, before bringing rain in August and especially in September. This climate favors the cultivation of *Vachelia nilotica* and *Senegalia senegal*, cotton, and cereals. Depending on the season, the landscape is characterized by savannah, grassland, and prickly steppe.

The exudates were collected and sun-dried at a temperature of 37°C for 21 days. Finally, the dried exudates were ground into a whitish water-soluble powder for easy storage and use.

### 2.2 ATR-FTIR Spectroscopy

The exudate extract powder was analyzed using a Perkin Elmer ATR Frontier spectrometer (Bruker Corporation, Epinal-France) equipped with a diamond/ZnSe crystal. The principle was to place about 2 mg of totally dry powder on the crystal device and contact was obtained by applying a force of about 150 N on the sample. Each spectrum was obtained with 32 scans with a resolution of 4 cm<sup>-1</sup> from 3500 to 400 cm<sup>-1</sup>.

### 2.3 Thermogravimetric Analysis

Thermogravimetric analysis (TGA) was carried out using NETZSCH STA 449F3 Jupiter equipment (Epinal-France). Approximately 100 mg of each cured sample of exudate extract powder was placed on a balance located in the oven and heat applied in the temperature range of 20 to 900°C at a heating rate of 5 °C/min for 60 min in argon. Mass losses were recorded on the TG curve and the mass loss rate on the DTG curve.

## 2.4 Desorption Study at Different Temperatures

Dynamic desorption experiments were performed as follows: 10 g of anhydrous rendered exudate powders were weighed using a digital balance (PGW 753i) with an accuracy of 1:1000e. Isotherms of 50°C, 70°C, 90°C, and 103°C were used for the experiments [32]. To achieve hygroscopic equilibrium with the environment, the specimens were kept in the laboratory in a controlled atmosphere with a relative humidity of 65% and a temperature of 24°C. The ventilated DRY OVER oven at the “Centre de Formation Professionnelle d’Excellence” (CFPE) in Douala was turned on and idled until stabilized before the samples were introduced. The samples were weighed to determine their wet mass  $m_i$  due to exposure in the laboratory before cooking. After every 5 min (t) in the oven, the m(t) value of the sample mass was recorded. This was repeated until the stabilized mass was recorded,  $m_f$  [33,34].

The desorption ratio, denoted MR, was determined using Eq. (1).

$$MR = \frac{m(t) - m_i}{m_f - m_i} \quad (1)$$

with:

m(t): sample mass

$m_i$ : wet mass

$m_f$ : stabilized mass

MR: desorption ratio

After desorption, the results of the analyses were used to plot the curves for the different temperatures and according to the mathematical models (Table 1). The mathematical models used, and their obtained correlation coefficient are presented in Tables 2 and 3 below.

**Table 1:** Mathematical models used in drying kinetics

Authors	Models	Reference
Newton et Lewis	$MR = \exp(-k*t)$	[35]
Page	$MR = \exp(-k*t^n)$	[36]
Henderson et pabis	$MR = a*\exp(-k*t)$	[37,38]
Logarithmic	$MR = a*\exp(-k*t) + b*t$	[38,39]
Two term	$MR = a*\exp(-k*t) + b*\exp(-kI*t)$	[38,40]
Midilli	$MR = a*\exp(-k*t) + b*t$	[41]
Verma et al.	$MR = a*\exp(-k*t) + (1-a)\exp(-g*t)$	[42,43]
Modifier Anderson et Pabis	$MR = a*\exp(-k*t) + b*\exp(-g*t) + c*\exp(-h*t)$	[44]
Peleg	$MR = 1 - [t(a + b*t)]$	[45]
Aghbashlo	$MR = \exp[-k*t/(1 + a*t)]$	[46]

The Newton and Lewis model is the general solution to the Fick equation, it only considers diffusion based on water migration. In 1949, Page modified the Lewis model to get a more accurate model by adding an empirical dimensionless constant (n) and applying this approach to grain drying [47]. Henderson et al. [40] improved the drying model by using Fick’s second law of diffusion and applying it to grain drying. In 1994, Prabir et al. [39] proposed a new model derived from the Henderson and Pabis model with the addition of an empirical term (Logarithmic). In 2002, Midilli et al. [41] proposed a new model with the addition of an additional empirical term incorporating time t to the Henderson and Pabis model. This new model is the combination of an exponential term and a linear term. They applied

this model to the drying of pollen, mushrooms, and pistachio for different drying methods. In 2001, Medeni Maskan applied the Peleg model to the drying of cereals, wheat, and firik (roasted/flame-cured immature wheat ears). The moisture content of the grains was about 09% [45].

**Table 2:** Comparison of the applicability of the models in the desorption kinetics of temperature 60°C, 70°C, 80°C, 90°C and 100°C

Temperatures			60°C	70°C	80°C	90°C	100°C
Statistical indicator			R <sup>2</sup>				
No.	Models	Number of parameters					
1	Newton et lawis	01	0.9668	0.9421	0.998	0.9896	0.9964
2	Page	02	0.9973	0.9934	0.9984	0.997	0.9992
3	Henderson et pabis	02	0.9803	0.962	0.9981	0.9926	0.9972
4	Logarithmic	03	0.9814	0.9667	0.9983	0.9927	0.9973
5	Two term	04	0.9898	0.9764	0.9982	0.998	0.9987
6	Midilli	04	0.9974	0.9941	0.9985	0.9979	0.9993
7	Ferma et al.	03	0.9976	0.9975	0.9991	0.9979	0.9987
8	Modifier Anderson et Pabis	06	0.9983	0.9988	0.9982	0.9989	0.9993
9	Peleg	02	0.9955	0.9973	0.9804	0.9969	0.9941
10	Aghbashlo	02	0.9964	0.9978	0.9987	0.9947	0.9987

**Table 3:** Calculated parameters of Anderson and Pabis model for desorption kinetics

Temperature	K	A	b	C	G	h
Desorption at T° 60°C	0.00188	0.08978	0.7037	0.2108	0.01239	6.69E-02
Desorption at T° 70°C	0.0161	0.6626	0.1652	0.1739	0.00197	6.52E-02
Desorption at T° 80°C	30.11	0.2358	0.9804	-0.2161	0.01809	1.20E+00
Desorption at T° 90°C	0.02918	-14.19	8.33	6.865	0.02425	3.50E-02
Desorption at T° 100°C	0.02187	0.3407	0.1992	0.4616	0.0798	2.28E-02

The models of Two-term, Midilli, Verma et al. [43], Modifier Anderson and Pabis, Peleg and Aghbashlo were compared in terms of their coefficients of determination to estimate the solar drying curves of prickly pear fruit in a convective solar dryer operated with an auxiliary heating system under air-controlled conditions. The model of prickly pear fruit in a convective solar dryer operating with an auxiliary heating system under air-controlled conditions was found to satisfactorily describe the solar drying curves of prickly pear fruit with a correlation coefficient(r) near 1 [38,46].

Desorption was performed at 60°C, 70°C, 80°C, 90°C and 100°C. The experimental results were compared with different mathematical models (Table 2) using Matlab software.

The model with the best correlation and lowest error can be selected from Table 3. It shows the average correlation coefficients of the different mathematical models.

The Modifier Anderson and Pabis model with the best correlation for all temperatures was chosen to predict water desorption from exudates. The model equation is  $MR = a*exp(-k*t) + b*exp(-g*t) + c*exp(-h*t)$  (Fig. 4) with the parameters shown in Tables 2 and 3.

## 2.5 Preparation of Particleboard

The pure maritime pine (*Pinus pinaster*) tannin extract used as the resin was obtained from DRT (Derivés Résiniques et Terpeniques, Dax, France) was characterized previously [48].

Identical monolayer particleboards were prepared and tested using the following adhesive mixture: 100 g of pure maritime pine (*Pinus pinaster*) tannin was dissolved in water to give a concentration of 40% to 45% solids. The pH was corrected to 7.5 with a NaOH solution at a concentration of 33%. To this were added 10% *Vachellia nilotica* powder extract as a bio-hardener on the tannin solids. The adhesive mixture was applied at a level of 10%, by weight of the total solids content of the adhesive (tannin + exudate hardener) calculated on dry industrial pine wood chips. The wood chips had a moisture content of 2%. The particleboards were hot-pressed at 220°C for 7.5 min with a pressure cycle of 2.7 MPa/1.47 MPa/0.5 MPa min respectively (Table 6). All prepared panels were 350 × 350 × 14 mm<sup>3</sup> in size. After cooling, each panel was conditioned at a temperature of 20°C and 65% relative humidity to reach an equilibrium moisture content of 12%, then cut and 5 samples of 50 × 50 mm for each panel was tested for internal bond strength (IB) in the dry state according to EN 319 [37]. It is known that evidence of bonding performance is best measured in particleboard by measuring the internal bond strength (IB). IB strength was measured at a separation rate of 2 s per mm and according to EN 319 [49]. Control panels using an industrial urea-formaldehyde (UF) resin (Georgia-Pacific LEAFC2 resin) with a urea/formaldehyde molar ratio of 1:1.08, a solids content of 66%, a viscosity at 20°C of 450 MPa.s, and a pH of 7.5, were also pressed under the same conditions with an IB = 0.40 MPa approximately. The adhesive was applied at the same level of total resin loading so that the results could be compared.

## 3 Results and Discussion

### 3.1 FTIR Analysis

Fig. 1 shows the FTIR spectrum of the extracts of different exudates: *Vachellia nilotica* or *Acacia Nilotica* (D67 series), *Vachellia seyal* or *Acacia Seyal* (D68 series), and *Senegalia senegal* (D69 series) (3 samples of exudates) studied in the fingerprint range (3500–400 cm<sup>-1</sup>).

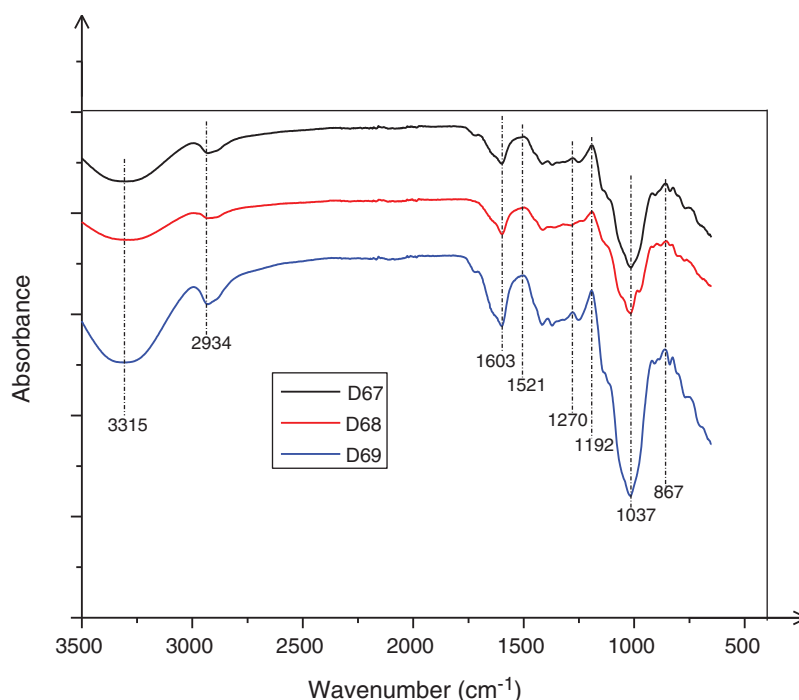


**Figure 1:** ATR-FT spectrum of the extract of *Senegalia senegal*, *Vachellia nilotica*, *Vachellia seyal*, *Acacia siebteriana* exudates between 3500 and 400 cm<sup>-1</sup>

Fig. 1 and Table 4 show absorption peaks and wavenumbers of the functional groups present in the exudate extracts used as hardeners. These are listed in Table 3.

Thus, as with the spectra of all the curves in Fig. 4, the broad absorption band at  $3315\text{ cm}^{-1}$ , is attributed to the aromatic and aliphatic -OH groups characteristic of the FT-IR spectrum of exudates. There are two bands at  $2934\text{ cm}^{-1}$  and  $1603\text{ cm}^{-1}$ , relative to the C-H stretching vibration of  $-\text{CH}_2$  and  $-\text{CH}_3$  [50]. Moreover, the peaks at  $1192$ ;  $1034$ ;  $1037$ , and  $1148\text{ cm}^{-1}$  common to the spectra of the different exudate extracts are assigned to the C-O stretching vibration of the ether groups, and the peaks  $1415$ ;  $1037\text{ cm}^{-1}$  correspond to the O-H bending vibration of the furans [51], the  $802$  and  $1521\text{ cm}^{-1}$  peaks are characteristics of furan rings [52]. The presence of elements of the sugar family has also been identified in these extracts. This presence is confirmed by the peaks at  $916$  and  $851\text{ cm}^{-1}$  which are attributed to the stretching of sucrose and fructose (C-C) and the values of  $831$  and  $851\text{ cm}^{-1}$  where the C-C-H deformation of hydroxymethylfurfural is affected. Thus, there are oligomers of different types all giving 5-hydroxy-2-hydroxymethylfuran and 2, 5-dihydroxymethylfuran (Fig. 2) which are then the true curing molecules [12]. By comparing the spectra of the different exudates, we observe that they can be interchangeable. There are C=O absorption peaks at  $1192\text{ cm}^{-1}$ . During the curing process, these will continue to form ether bonds (C-O-C) or methylene bridges ( $-\text{CH}_2-$ ) thus improving the bonding.

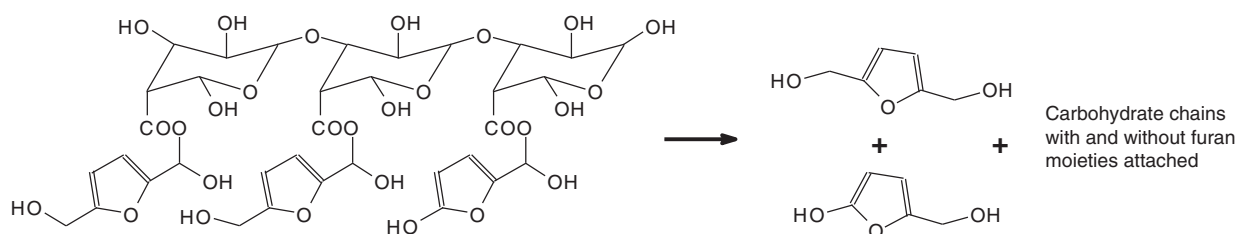


**Figure 2:** Formation of 2-hydroxy-5-hydroxymethyl furan

**Table 4:** Summary of bands present in exudate and associated assignments

Wavenumber ( $\text{cm}^{-1}$ )	Band assignment
802	Characteristic peak of the furan rings
831	Fructose C-C-H deformation of sucrose
851 (850)	C-C-H deformation anomer
867	C-C stretching of fructoses
916	C-C stretching of glucose
1034–1037	C-O; O-H bending vibration of glucose
1148	C-O Stretch
1192	Vibrations of the C-O stretches
1270	C-H deformation of sucrose
1415	C-H and O-H stretching of sorbitol
1521	Vibrations of the C=C stretches (aromatic furan ring)
2934 and 1603	C-H stretching vibration of $-\text{CH}_2$ and $-\text{CH}_3$
3315	Aromatic and aliphatic -OH groups

### 3.2 Thermogravimetric Analysis

To evaluate the thermal stability of *Vachellia nilotica*; *Senegalia senegal*, and *Vachellia seyal* exudates, the thermogravimetric analysis (TGA) curves are presented in Fig. 3. The corresponding specific degradation temperatures and char yields at 799°C are listed in Table 5.

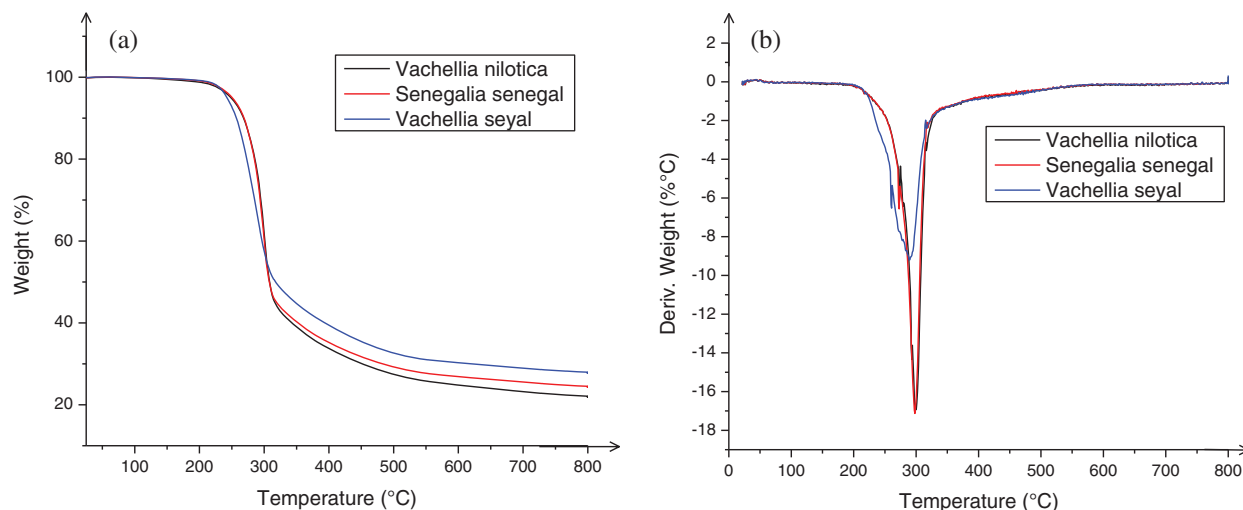


**Figure 3:** TGA (a) and Derivative Thermogravimetry (DTG) (b) curves of different exudates used as bio-hardeners (under N<sub>2</sub> atmosphere)

**Table 5:** Thermo analytical data of bio-hardeners

Samples	Areas of degradation (°C)	Peak temperature (°C)	Residual mass (%)
exudate of <i>Vachellia nilotica</i>	25–140	126.6	22.1
	140–520	312.4	
	520–799.2	799.2	
exudate of <i>Senegalia senegal</i>	25–170	126.5	24.5
	170–510	312.4	
	510–798.9	798.9	
exudate of <i>Vachellia seyal</i>	25–200	126.9	27.8
	200–470	304.9	
	470–798.3	798.3	

Similar three-step pyrolysis behavior of the exudates is observed in Fig. 3. The initial weight loss occurs in the temperature range of 25°C and 140, 170, 200°C for the exudate extracts of *Vachellia nilotica*, *Senegalia senegal* and *Vachellia seyal* respectively 25°C and 140, 170, 200°C for the exudate extracts of *Vachellia nilotica*, *Senegalia senegal* and *Vachellia seyal*, this being related to the release of volatilized absorbed water [40]. For this region, the decomposition peak around 126°C is due to the degradation of the exudate extracts side chains [53]. In this step, a weight loss of 0.29% occurred for the exudate of *Vachellia nilotica*, while a weight loss of 0.20% occurred for the exudates of *Senegalia senegal* and *Vachellia seyal*. The second range of weight loss is between 140°C and 520°C for *Vachellia nilotica*, between 170°C and 200°C showing 52.98% weight loss for exudates of *Vachellia nilotica* and

*Vachellia seyal*, 45.37 weight loss for exudates of *Senegalia senegal*. The weight loss in this range is related to decomposition reactions by cleavage of intermolecular bonds; it is due to the decomposition of the rigid segments of the exudates on the one hand and a release of CO, CO<sub>2</sub>, and CH<sub>4</sub> on the other hand. The third weight loss is the stage of exudate decomposition. This is the stage where the last weight loss occurs, which is greater than 30%. These results show that the exudates show similar weight losses at the pyrolysis temperature. Nevertheless, a slight difference exists in the residual mass at 799°C of the different types of exudates produced. The residual masses are of 22.1% for the exudate of *Vachellia nilotica*, 24.5% for the exudate of *Senegalia senegal* and 27.8% for the exudate of *Vachellia seyal*. The results show that the exudates have such high residues. On the one hand, this may mean that they have high flammability, a longer burning time, and higher burning intensity. On the other hand, it could be explained by their richness in secondary metabolites. Thermal stability has been observed at around 200°C.

From the analysis of Table 5, the residue value shows that the exudate of *Vachellia seyal* lost less mass than the other two, followed respectively by the exudate of *Senegalia senegal* and *Vachellia nilotica* as follows (27.8 > 24.5 > 22.1%). The onset of decomposition of the biohardeners (25°C) is identical for all extracts; the thermal stability was observed around 200°C. The impurity of the compounds explains their strong decomposition. The pyrolysis curves of *Vachellia nilotica* exudate, *Senegalia senegal* exudate and *Vachellia seyal* exudate (Fig. 3) reveal that the major difference in the decomposition of these biohardeners is very small, which means that they can be superimposed on each other. The difference in decomposition observed in the temperature range of 300°C–750°C would be due to their thermal stability at high temperatures. Indeed, the chemical elements contained in these different bio hardeners such as fructose, sucrose, and furan (Table 3) with melting points of 103, 186, and –85.6°C respectively do not degrade in the same way at high temperature.

### 3.3 Desorption at 60°C, 70°C, 80°C, 90°C, and 100°C

To predict the behavior of bio-hardeners both in the development of liquid-bonded composites and in the face of hydric environmental conditions and to harmonize their curing methods, the adopted Modifier Anderson and Pabis model were used to plotting and compare the desorption curves at 60°C, 70°C, 80°C, 90°C and 100°C (Fig. 4). A similar evolution of MR is observed for the time interval from 0 to 30 min.

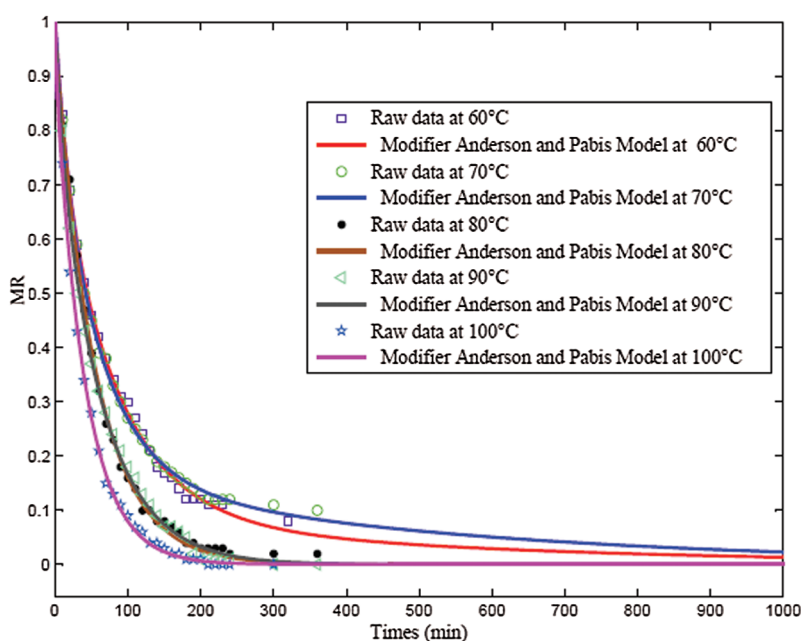


**Figure 4:** Desorption curves for the different temperatures 60°C, 70°C, 80°C, 90°C, and 100°C according to the Anderson and Pabis Modifier model

**Table 6:** Results of laboratory particleboard bonded with exudate bio-hardeners and UF

Press time (minutes)	Density (kg/m <sup>3</sup> )	Dry IB strength (MPa)	pH	Exudate of <i>Vachellia nilotica</i> (%)	Dry IB strength (UF) (MPa)
7.5	707	0.42 + 0.05	7.5	10	0.44 + 0.03
7.5	711	0.42 + 0.03	7.5	10	0.45 + 0.05
7.5	704	0.41 + 0.03	7.5	10	0.43 + 0.03
7.5	707	0.42 + 0.03	7.5	10	0.45 + 0.05

Beyond 30 min, the desorption kinetics at 60°C and 70°C became slower than those at 80°C, 90°C, and 100°C; the dry state was reached in 90 min for 100°C, in 100 min for temperatures 80°C and 100°C, and in 200 min at 60°C and 70°C. For the 80°C and 90°C kinetics, there was a trend toward stabilization around 180 min.

The study showed the thermal stability of the exudates for temperatures up to the boiling temperature of water of 100°C; the samples did not show any form of cracking or degradation. It is an advantage to use this bioresource as a bio-hardener to elaborate panel resins usable in furniture, in thermal insulation and acoustics, and as structuring materials. Thus, it is also possible to use it as aggregate for paints and anti-corrosives. Thus, it would be interesting to use it in the form of vessels or particles and the form of sand respectively for their use in wood composites and the manufacture of abrasives.

### 3.4 Comparative Bonding Test of Particleboard

The encouraging dry IB strength values obtained for particleboard using the bio-hardeners (Table 6) indicate that these extracts are ideal for interior grade adhesives, along with those using paraformaldehyde as a synthetic hardener under the same conditions.

These results show that it is possible to manufacture fully bio-based panels using the exudate extract of the African trees *Vachellia nilotica*, *Senegalia senegal*, and *Vachellia seyal* bio-hardener. The mechanical characteristics of these panels comply with European standards.

## 4 Conclusion

The development of a multifunctional renewable product that can prevent pollution, resist mold and fire has become a major research topic for wood modification at present. In this paper, exudates of *Vachellia nilotica*, *Senegalia senegal*, and *Vachellia seyal* from Cameroonian renewable biomass were extracted for use as 100% bio-hardeners of tannin matrix particleboard for the wood industry in this study. The results showed that these bio-hardeners composed mainly of reactive species known as 2, 5-hydroxymethyl furan linked to carbohydrate oligomers:

- Represent a good future alternative for the wood industry, as the heat resistance of various species is encouraging. The biggest difference between these formulations occurs around 300°C.
- For the absorption kinetics, among the 10 models tested, the model Modifier Anderson and Pabis was the best mathematical model for the prediction of the phenomenon. The study kinetics study showed the thermal stability of exudates for temperatures up to 100°C.
- Particleboard using exudates as a biohardener showed satisfactory internal bond strength as particleboard that was cured with paraformaldehyde.

From all the results obtained, exudates are found to be very effective as fire retardants in case of fire. Therefore, this approach is applicable in practice.

**Acknowledgement:** The authors would like to thank Gabriel Maila and Wadjore Abdoulaye for their participation in the laboratory activities.

**Funding Statement:** The authors received no specific funding for this study.

**Conflicts of Interest:** The authors declare that they have no conflicts of interest to report regarding the present study.

## References

1. Kadja, K., Drovou, S., Kassegne, K. A., Pizzi, A., Sanda, K. et al. (2019). Development and investigation into properties of composite particleboard of iroko and african locust bean Pod. *Procedia Manufacturing*, 30, 188–193. DOI 10.1016/j.promfg.2019.02.027.
2. Jingbin, T. Y. Y. W. J., Dadi, L. G. Y. (1991). Development of larch bark powder modified phenol-formaldehyde resin adhesive. *Journal of Jilin Forestry University*, 3.
3. Golling, F. E., Pires, R., Hecking, A., Weikard, J., Richter, F. et al. (2019). Polyurethanes for coatings and adhesives—chemistry and applications. *Polymer International*, 68(5), 848–855. DOI 10.1002/pi.5665.
4. Pizzi, A. (2006). Recent developments in eco-efficient bio-based adhesives for wood bonding: Opportunities and issues. *Journal of Adhesion Science and Technology*, 20(8), 829–846. DOI 10.1163/15685610677638635.
5. Pichelin, F., Nakatani, M., Pizzi, A., Wieland, S., Despres, A. et al. (2006). Structural beams from thick wood panels bonded industrially with formaldehyde-free tannin adhesives. *Forest Products Journal*, 56(5), 31.
6. Liu, Y., Li, K. (2007). Development and characterization of adhesives from soy protein for bonding wood. *International Journal of Adhesion and Adhesives*, 27(1), 59–67. DOI 10.1016/j.ijadhadh.2005.12.004.
7. Konai, N., Pizzi, A., Raidandi, D., Lagel, M., L’Hostis, C. et al. (2015). Anigre (*Aningeria* spp.) tannin extract characterization and performance as an adhesive resin. *Industrial Crops and Products*, 77, 225–231. DOI 10.1016/j.indcrop.2015.08.053.
8. Abdullah, U. H. B., Pizzi, A. (2013). Tannin-furfuryl alcohol wood panel adhesives without formaldehyde. *European Journal of Wood and Wood Products*, 71(1), 131–132. DOI 10.1007/s00107-012-0629-4.
9. Delgado-Sánchez, C., Santiago-Medina, F., Fierro, V., Pizzi, A., Celzard, A. (2018). Optimisation of “green” tannin-furanic foams for thermal insulation by experimental design. *Materials & Design*, 139, 7–15. DOI 10.1016/j.matdes.2017.10.064.
10. Ndiwe, B., Tibi, B., Danwe, R., Konai, N., Pizzi, A. et al. (2020). Reactivity, characterization and mechanical performance of particleboards bonded with tannin resins and bio hardeners from african trees. *International Wood Products Journal*, 11(2), 80–93. DOI 10.1080/20426445.2020.1731070.
11. Ndiwe, B., Pizzi, A., Tibi, B., Danwe, R., Konai, N. et al. (2019). African tree bark exudate extracts as biohardeners of fully biosourced thermoset tannin adhesives for wood panels. *Industrial Crops and Products*, 132, 253–68. DOI 10.1016/j.indcrop.2019.02.023.
12. Ndiwe, B., Pizzi, A., Danwe, R., Tibi, B., Konai, N. et al. (2019). Particleboard bonded with bio-hardeners of tannin adhesives. *European Journal of Wood and Wood Products*, 77(6), 1221–3. DOI 10.1007/s00107-019-01460-5.
13. Owodunni, A. A., Lamaming, J., Hashim, R., Taiwo, O. F. A., Hussin, M. H. et al. (2020). Adhesive application on particleboard from natural fibers: A review. *Polymer Composites*, 41(11), 4448–4460. DOI 10.1002/pc.25749.
14. Adhikari, B., Appadu, P., Kislitsin, V., Chae, M., Choi, P. et al. (2016). Enhancing the adhesive strength of a plywood adhesive developed from hydrolyzed specified risk materials. *Polymers*, 8(8), 285. DOI 10.3390/polym8080285.
15. Antov, P., Savov, V. (2019). Possibilities for manufacturing eco-friendly medium density fibreboards from recycled fibres—a review. *30th International Conference on Wood Science and Technology, ICWST 2019 and 70th Anniversary of Drvna Industrija Journal: Implementation of Wood Science in Woodworking Sector, Proceedings, Zagreb, Croatia*.
16. Veigel, S., Rathke, J., Weigl, M., Gindl-Altmutter, W. (2012). Particle board and oriented strand board prepared with nanocellulose-reinforced adhesive. *Journal of Nanomaterials*, 212, 158503. DOI 10.1155/2012/158503.

17. Čuk, N., Kunaver, M., Poljanšek, I., Ugovšek, A., Šernek, M. et al. (2015). Properties of liquefied wood modified melamine-formaldehyde (MF) resin adhesive and its application for bonding particleboards. *Journal of Adhesion Science and Technology*, 29(15), 1553–1562. DOI 10.1080/01694243.2015.1034924.
18. Hemmilä, V., Adamopoulos, S., Hosseinpourpia, R., Ahmed, S. A. (2019). Ammonium lignosulfonate adhesives for particleboards with pMDI and furfuryl alcohol as crosslinkers. *Polymers*, 11(10), 1633. DOI 10.3390/polym11101633.
19. Kevin, E. I., Ochanya, O. M., Olukemi, A. M., Bwanhot, S. T. N., Uche, I. (2018). Mechanical properties of urea formaldehyde particle board composite. *American Journal of Chemical and Biochemical Engineering*, 2(1), 10–15. DOI 10.11648/j.ajcbe.20180201.12.
20. Pizzi, A. (2003). Melamine-formaldehyde Adhesives. In: *Handbook of adhesive technology*, vol. 2.
21. Boran, S., Usta, M., Gümüşkaya, E. (2011). Decreasing formaldehyde emission from medium density fiberboard panels produced by adding different amine compounds to urea formaldehyde resin. *International Journal of Adhesion and Adhesives*, 31(7), 674–678. DOI 10.1016/j.ijadhadh.2011.06.011.
22. Liu, J., Yue, K., Xu, L., Wu, J., Chen, Z. et al. (2020). Bonding performance of melamine-urea–formaldehyde and phenol-resorcinol-formaldehyde adhesive glulams at elevated temperatures. *International Journal of Adhesion and Adhesives*, 98, 102500. DOI 10.1016/j.ijadhadh.2019.102500.
23. Mamza, P. A., Ezeh, E. C., Gimba, E., Arthur, D. E. (2014). Comparative study of phenol formaldehyde and urea formaldehyde particleboards from wood waste for sustainable environment. *International Journal of Scientific & Technology Research*, 3(9), 53–61.
24. Santiago-Medina, F. -J., Pizzi, A., Abdalla, S. (2017). Hydroxymethylfurfural hardening of pine tannin wood adhesives. *Journal of Renewable Materials*, 5(5), 435–447. DOI 10.7569/JRM.2017.634166.
25. Evon, P., Kartika, I. A., Rigal, L. (2014). New renewable and biodegradable particleboards from *Jatropha* press cakes. *Journal of Renewable Materials*, 2(1), 52–65. DOI 10.7569/JRM.2013.634131.
26. Papadopoulou, E., Chrissafis, K. (2017). Particleboards from agricultural lignocellulosics and biodegradable polymers prepared with raw materials from natural resources. In: *Natural fiber-reinforced biodegradable and bioresorbable polymer composites*. Elsevier; <https://linkinghub.elsevier.com/retrieve/pii/B9780081006566000029>.
27. Lambert, J. B., Donnelly, E. W., Heckenbach, E. A., Johnson, C. L., Kozminski, M. A. et al. (2013). Molecular classification of the natural exudates of the rosids. *Phytochemistry*, 94, 171–183. DOI 10.1016/j.phytochem.2013.06.013.
28. Ndinga, E. M. A. (2015). *Inventory and chemical analysis of exudates of commonly used plants in Congo-Brazzaville (Thesis)*. Université Paris-sud.
29. Bruneton, J., Massiot, G. (1994). Pharmacognosie: Phytochimie, plantes médicinales. *Phytochemistry*, 36(1), 258. DOI 10.1016/S0031-9422(00)97054-7.
30. Junior, V. V., Rosas, E., Carvalho, M. V., Henriques, M. G. M. O., Pinto, A. C. (2007). Chemical composition and anti-inflammatory activity of copaiba oils from *copaifera cearensis huber ex ducke*, *copaifera reticulata ducke* and *copaifera multijuga hayne*—A comparative study. *Journal of Ethnopharmacology*, 112(2), 248–254. DOI 10.1016/j.jep.2007.03.005.
31. Onana, J. M. (2018). Cartographie des écosystèmes du cameroun. *International Journal of Biological and Chemical Sciences*, 12(2), 940–957. DOI 10.4314/ijbcs.v12i2.25.
32. Nguyen, T. H. (2015). *Étude expérimentale et modélisation du procédé de séchage des végétaux (Ph.D. Thesis)*. Université de Bretagne Sud.
33. Mao, J., Lin, S., Lu, X. J., Wu, X. H., Zhou, T. et al. (2020). Ion-imprinted chitosan fiber for recovery of Pd(II): Obtaining high selectivity through selective adsorption and two-step desorption. *Environmental Research*, 182, 108995. DOI 10.1016/j.envres.2019.108995.
34. Bhatti, H. N., Safa, Y., Yakout, S. M., Shair, O. H., Iqbal, M. et al. (2020). Efficient removal of dyes using carboxymethyl cellulose/alginate/polyvinyl alcohol/rice husk composite: Adsorption/desorption, kinetics and recycling studies. *International Journal of Biological Macromolecules*, 150, 861–870. DOI 10.1016/j.ijbiomac.2020.02.093.

35. Sander, A. (2007). Thin-layer drying of porous materials: Selection of the appropriate mathematical model and relationships between thin-layer models parameters. *Chemical Engineering and Processing: Process Intensification*, 46(12), 1324–1331. DOI 10.1016/j.cep.2006.11.001.
36. Page, G. E. (1949). *Factors influencing the maximum rates of air drying shelled corn in thin layers*, (M.S. Thesis). Agricultural Engineering, Purdue University.
37. Henderson, S., Pabis, S. (1962). Grain drying theory: IV. the effect of air flow rate on the drying index. *Journal of Agricultural Engineering Research*, 7(2), 85–89.
38. Lahsasni, S., Kouhila, M., Mahrouz, M., Jaouhari, J. (2004). Drying kinetics of prickly pear fruit (*Opuntia ficus indica*). *Journal of Food Engineering*, 61(2), 173–179. DOI 10.1016/S0260-8774(03)00084-0.
39. Chandra, P. K., Singh, R. P. (1994). *Applied numerical methods for food and agricultural engineers*. Boca Raton, Florida, USA: CRC Press.
40. Henderson, S. (1974). Progress in developing the thin layer drying equation. *Transactions of the ASAE*, 17(6), 1167–1168. DOI 10.13031/2013.37052.
41. Midilli, A., Kucuk, H., Yapar, Z. (2002). A new model for single-layer drying. *Drying Technology*, 20(7), 1503–1513. DOI 10.1081/DRT-120005864.
42. Doymaz, I. (2007). The kinetics of forced convective air-drying of pumpkin slices. *Journal of Food Engineering*, 79(1), 243–248. DOI 10.1016/j.jfoodeng.2006.01.049.
43. Verma, L. R., Bucklin, R., Endan, J., Wratten, F. (1985). Effects of drying air parameters on rice drying models. *Transactions of the ASAE*, 28(1), 296–301. DOI 10.13031/2013.32245.
44. Karathanos, V. T. (1999). Determination of water content of dried fruits by drying kinetics. *Journal of Food Engineering*, 39(4), 337–344. DOI 10.1016/S0260-8774(98)00132-0.
45. Maskan, M. (2002). Effect of processing on hydration kinetics of three wheat products of the same variety. *Journal of Food Engineering*, 52(4), 337–341. DOI 10.1016/S0260-8774(01)00124-8.
46. Aghbashlo, M., Kianmehr, M., Khani, S., Ghasemi, M. (2009). Mathematical modelling of thin-layer drying of carrot. *International Agrophysics*, 23(4), 313–317.
47. Erbay, Z., Icier, F. (2010). A review of thin layer drying of foods: Theory, modeling, and experimental results. *Critical Reviews in Food Science and Nutrition*, 50(5), 441–464. DOI 10.1080/10408390802437063.
48. Navarrete, P., Pizzi, A., Pasch, H., Rode, K., Delmotte, L. (2013). Characterization of two maritime pine tannins as wood adhesives. *Journal of Adhesion Science and Technology*, 27(22), 2462–2479. DOI 10.1080/01694243.2013.787515.
49. BS EN 319:1993. Particleboards and fibreboards. Determination of tensile strength perpendicular to the plane of the board. (1993).
50. Zhou, F., Zhang, T., Zou, B., Hu, W., Wang, B. et al. (2020). Synthesis of a novel liquid phosphorus-containing flame retardant for flexible polyurethane foam: Combustion behaviors and thermal properties. *Polymer Degradation and Stability*, 171, 109029. DOI 10.1016/j.polymdegradstab.2019.109029.
51. Bureau, S., Cozzolino, D., Clark, C. J. (2019). Contributions of Fourier-transform mid infrared (FT-MIR) spectroscopy to the study of fruit and vegetables: A review. *Postharvest Biology and Technology*, 148, 1–14. DOI 10.1016/j.postharvbio.2018.10.003.
52. Xi, X., Liao, J., Pizzi, A., Gerardin, C., Amirou, S. et al. (2019). 5-Hydroxymethyl furfural modified melamine glyoxal resin. *The Journal of Adhesion*, 96(13), 1167–1185. DOI 10.1080/00218464.2018.1561291.
53. Branca, C., Blasi, C. D., Russo, C. (2005). Devolatilization in the temperature range. 300–600 K of liquids derived from wood pyrolysis and gasification. *Fuel*, 84(1), 37–45.